Research Article

Approaches to tailor the cooling supply to the grinding process

Berend Denkena[1] · Benjamin Bergmann[1] · Tobias Gartzke[1] · Michael Wilckens[1]

© The Author(s) 2022   OPEN

Abstract

This study presents original research of the investigation of the coolant supply to the contact area with two different approaches. The cooling and lubrication are key aspects of manufacturing processes such as grinding to achieve a high surface quality at high productivity. The coolant supply to the contact area has a high impact on the performance of the coolant. This paper presents the results from two approaches to tailoring the coolant supply for conventional and high-performance processes. An analytical approach is established to determine the coolant outlet velocity. Afterward, a sensor is developed to measure the coolant velocity at the nozzle. Conclusively, the influence of the coolant velocity on the volume flow through the contact zone is investigated. The results of this study highlight the importance of coolant outlet velocities of at least 60% of the cutting speed. The two approaches outline low impact possibilities to ensure optimal coolant outlet velocities and thus low thermal loads during the grinding process.

Article Highlights

- Analytical approach to calculate outlet velocities for varying noozles in high-performance grinding with cutting speeds of up to 100 m/s
- Utilization of a high-speed camera to determine the outlet nozzle velocities in a conventional deep grinding process

- Validation of the impact of the coolant outlet velocity on the volume flow through the contact area by means of a coolant collection box

1 Introduction

The use of cooling lubricant (coolant) serves multiple purposes during the grinding process. The first is the lubrication of the tool-workpiece contact. The reduction of friction reduces the heat generation during the process. The cooling effect, on the other hand, removes generated heat from the contact area. Other effects of the coolant are the chip removal from the contact zone and the chip

space of the tool and corrosion prevention. Oil- and water-based coolants are the two most commonly used fluids in machining today. Grinding oil has a higher capacity to reduce friction between the grinding wheel surface and the workpiece. Water-based cooling emulsions have a higher heat capacity and are therefore well suited to remove high amounts of heat from the contact area [1, 2].

As a result, the industrial common use of oil as a coolant leads to a relatively lower surface roughness but also to

---

a higher tendency to resulting tensile residual stresses [3]. Subsequently, the grinding process can be optimized by the choice of the fluid type. Further developments on coolant fluids are the minimum quantity lubrication, the cryogenic cooling [4] as well as solid-phase additives such as graphite nanoflakes [5]. The objective of these developments is the increase in lubrication and/ or cooling of the process. However, drawbacks of such developments are additional drive and filtering units as well as protective units, e.g. gas detectors [6, 7]. Therefore, the choice of coolant has to be made in most cases at the stage of production of the grinding machine tool. While a change between e.g. oils can be done technically with ease, a change from oil to emulsion leads to increased retrofitting costs due to additional components. In the case of existing grinding machines, the main optimization approach is the adaption of coolant conditions to the cutting conditions i.e. the feed of coolant into the contact zone as well as the capacity for coolant in the contact zone [8]. With the proper coolant conditions, the material separation process is optimized so that higher cutting speeds and overall higher removal rates can be achieved [9, 10].

For the coolant to reach the contact area, however, it has to overcome the air cushion that surrounds the rotating grinding wheel (Fig. 1). The rotation leads to two separate air flows. As air particles are accelerated with the tools rotation, a circumferential air flow is induced (Couette flow) as well as an air flow that is sucked toward the front surfaces of the grinding wheel. These air flows lead to turbulences along the circumference of the tool and interfere with the coolant supply to the contact area [9, 11–13]. To ensure proper cooling conditions, these turbulences have to be overcome or shielded. It has been proven, that the optimal nozzle outlet velocity for the coolant in grinding should equal the cutting speed v_c [14–16].

In addition, the coolant velocity v_{cool} can be adjusted to the circumferential speed of the grinding wheel so that the

Wi/106235 © IFW

Fig. 1 Mantle of air surrounding the grinding wheel [13]

coolant does not need to be accelerated after the nozzle outlet in order to get into the contact zone. This is based on a tangential orientation of the coolant beam to the grinding wheel and orientation of both speeds in the same direction. An optimal ratio v_{cool}/v_s has been examined in various papers [17–19]. Accordingly, the first contact of the coolant beam with the grinding wheel occurs from $v_{cool}/v_s = 0.6$ [19]. The optimum ratio can be narrowed down to a range of 0.8 to 1.0. By means of such an optimized process cooling, a large part of the process heat is dissipated via chips and coolant [20].

The coolant velocity can be adjusted through two main control variables of the pump conditions. On the one hand, the supply pressure through the coolant pump influences the pressure in front of the coolant nozzle [14]. Typical supply pressures of the pumps are in the range < 80 bar and mostly 10–30 bar. Common supply rates are 20–200 l/min [21]. However, high supply rates do not lead to an increase in the cooling effect from a process-specific saturation of the contact zone. This is already achieved at low values of less than 35 l/min if the speed ratio is maintained [17]. On the other hand, the change in the cross-section of the nozzle leads to a change in the flow rate due to mass continuity.

The major influence of the coolant conditions during grinding processes has been acknowledged by numerous researchers and ideal conditions were defined. Low-impact systems for measuring and adjusting the cooling conditions to the grinding process allow for better utilization of these benefits in an industrial context. The integration of such systems into existing machine tools is not widely done. This paper will show applicable components and methods for further industrial and scientific use.

The tailoring of coolant conditions by means of both, pump condition as well as nozzle specification is therefore subject to investigation throughout this paper. The influence of the nozzle geometry on the outlet velocity under varying pump conditions and nozzle setups is investigated in the first step. An analytical approach is used to improve the coolant conditions for a high-performance cylindrical grinding process with CBN tools to determine the maximum outlet velocities and flow rates. The influence of the ratio between cutting speed and coolant velocity has recently been shown for high efficient deep grinding processes by Zhang et al. [22]. To adjust the coolant conditions during the grinding process, a measuring system is implemented for in-process use. The validation of the ideal coolant conditions stated by Ott and Schnödt and their benefits for the grinding process is realized for a conventional grinding process at lower cutting speeds [19, 20]. Here, a new measuring method is introduced to determine the actual coolant outlet velocity by means of an adapted anemometer. With this, the influence of the speed ratio between the cutting speed and outlet velocity on the coolant flow rate through the contact zone
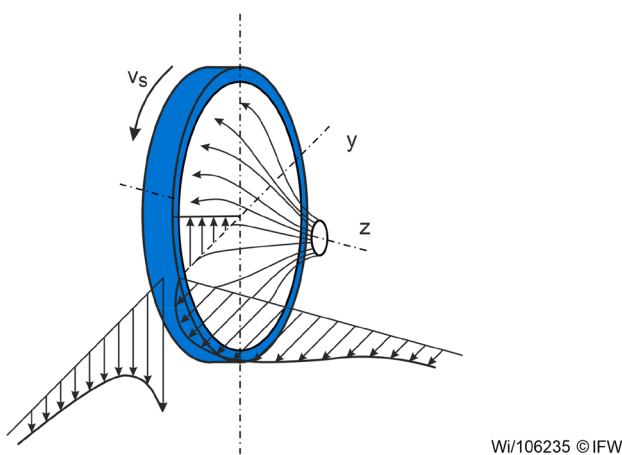
is shown for the conventional grinding process, to validate the measurement systems.

This paper is structured as follows: Chapter 2 presents the theoretical background of the analytical approach as well as the experimental setup for the implementation of an anemometer to measure the coolant velocity and the coolant flow through the contact area with a coolant collection box. Afterward, chapter 3 focuses on the measured coolant velocities for both processes and the influence of the coolant velocity on the chip temperatures. Finally, chapter 4 presents the conclusions and outlook of the study.

2 Materials and methods

2.1 Analytical approach

In the first step, the coolant velocity is calculated in an analytical approach. Based on this approach, the coolant supply can be tailored to the need of any given grinding process. Throughout this approach, the nozzle outlet velocity is calculated for multiple, different nozzle outlets based on Bernoulli's equation in fluid dynamics [Eq. (1)]. This equation is based on the theory of laminar flow and the principle of conservation of energy. This states that the sum of all forms of energy along laminar streamlines remains constant for all points along that streamline [21]. With the assumption of steady and incompressible flow properties and negligible viscous friction forces, the kinetic, internal, and potential energy between two points along the same coolant supply hose can be calculated. The equation shows the kinetic, internal and potential energy in terms of pressure. With the fluids density ρ and its velocity c its kinetic energy is calculated. The internal energy is represented by measured internal pressure p and the static pressure is calculated by the density ρ, the gravitational acceleration g and the elevation z.

$$\frac{1}{2}\rho c_1^2 + p_1 + \rho g z_1 = \frac{1}{2}\rho c_2^2 + p_2 + \rho g z_2 \qquad (1)$$

Additionally, the continuity equation states, that the rate at which fluid enters a system needs to be equal to the speed at which it exits the same system with the addition of the accumulation of fluid within the system [21]. With the cross-section A_1, the fluid velocity c_1 and the fluid's density $\rho_1 = \rho_2 = \rho$ at the coolant system entry known, the outlet velocity c_2 is calculated with the outlet cross-section A_2.

$$A_1 \cdot c_1 \cdot \rho_1 = A_2 \cdot c_2 \cdot \rho_2 = Q = konst. \qquad (2)$$

Based on the Hagen-Poiseuille principle of laminar fluid, Heinzel developed a calculation model for the coolant flow into the contact area [Eq. (3)]. The equation combines the tool induced drag of the fluid with

pressure gradient along the grinding gap. The fluid drag results from the thickness (h) of the fluid layer on the width of the grinding wheel (b) with a cutting speed v_c. The pressure gradient dp/dx on the other hand is dependent on the width and high of the grinding gap and the viscosity of the coolant η [9].

$$Q = v_c \cdot \frac{b \cdot h}{2} - \frac{dp}{dx} \cdot \frac{b \cdot h^3}{12 \cdot \eta} \qquad (3)$$

In order to calculate the coolant outlet velocities for different nozzle dimensions, flow rate and pressure sensors were integrated into the existing coolant supply system on a Schaudt CR41 cylindrical grinding machine. The used coolant is a grinding oil Castrol Variocut G600 HC with a density of $\rho = 0,849$ g/cm^3 (at 15 °C). A high-pressure pump PSA 1814 of the Spandau Pumps company is used to supply two different coolant nozzles. The primary nozzle cools the contact zone while the secondary nozzle extinguishes emitting sparks at the tool´s exit point. As both nozzles are fed from the same pump, the partial nozzle pressures p_{prim} and p_{sec}, the pump pressure p_{pu} and the flow rate of the pump Q_{pu} need to be measured. For this purpose, a flow rate meter SU9004 and three pressure meters (two PU5443 and PT9542) from ifm electronic GmbH are integrated into the existing coolant system according to Fig. 2. The flow rate meter SU9004 and pressure meter PT9542 were integrated immediately at the coolant pump, while the pressure meters for both nozzles (PU5443) were integrated about 20 cm before the nozzle outlet. For the variation of the nozzle outlet velocity, three different primary nozzles were investigated. Two flat-jet nozzles with an outlet of $A_{prim.} = 0.4 \cdot 18 = 7.2$ mm^2 and $A_{prim.} = 1 \cdot 18 = 18$ mm^2 and one needle nozzle with 8 separate needles with a diameter of $d = 2$ mm and an overall outlet of $A_{prim.} = 25.13$ mm^2 were used (Fig. 3). The secondary, extinguishing nozzle was not varied and has an outlet of $A_{sec.} = 88$ mm^2. For the investigation of the influence of the nozzle geometry on the outlet velocity and coolant flow rate into the contact area, the resulting partial pressures of the nozzles were measured and each outlet velocity was calculated.
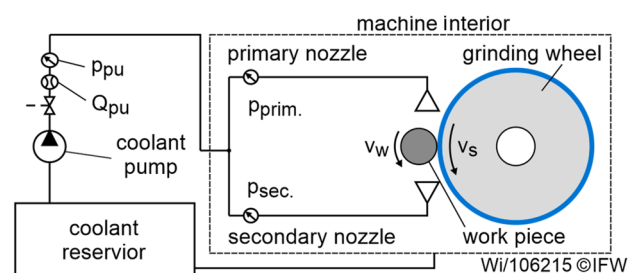

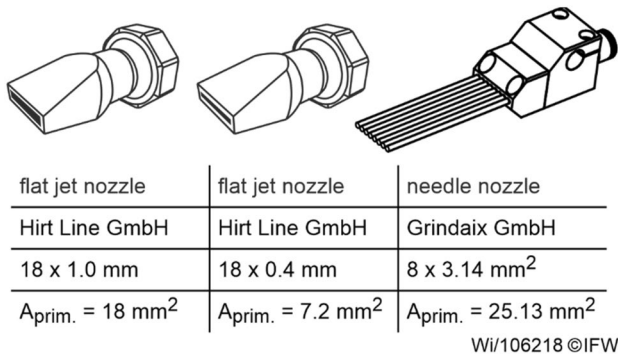**Fig. 2** Coolant supply for the Schaudt CR41 machine tool

flat jet nozzle	flat jet nozzle	needle nozzle
Hirt Line GmbH	Hirt Line GmbH	Grindaix GmbH
18 x 1.0 mm	18 x 0.4 mm	8 x 3.14 mm^2
$A_{prim.}$ = 18 mm^2	$A_{prim.}$ = 7.2 mm^2	$A_{prim.}$ = 25.13 mm^2

Wi/106218 ©IFW

Fig. 3 Investigated primary nozzles

Table 1 Essential specifications of the anemometer [22]

Feature	Unit	Value, range
Type	–	PCE-FST 200–201
Output signal U_a	V	0–10
Measurement range (air)	m/s	0–50
Accuracy (air)	m/s	±0,5
Maximum speed (air)	m/s	70
Ingress protection code	–	IP65

2.2 Experimental setup for conventional grinding processes

To examine the influence of the coolant outlet velocity on the grinding process, an experimental investigation was conducted on a KAPP KX1 that uses the same coolant as the Schaudt CR41 of the first part of this study. This allows the examination of the influence of the outlet velocity on the coolant flow through the contact zone. Within the investigation, a sensor is developed which is able to measure the actual coolant velocity and thus adjust it within the machine tool (Fig. 5). This sensor is based on an anemometer from PCE Instruments UK Ltd. in which a fluid flow causes the rotation of the sensor. The specifications of the sensor are shown in Table 1. For conventional use of the anemometer in measuring wind speed, a linear calibration is given. The change in the surrounding fluid flow required a new calibration. This was done by examining the coolant beam with a high-speed camera from the manufacturer Photron Fastcam, type SA5. By means of the high-speed camera, it is possible to observe the coolant jet through a plexiglass pane without coolant escaping from the machine (Fig. 4). The illumination was provided by three externally positioned spotlights, which ensures sufficient exposure of the camera even at short shutter speeds. The coolant nozzle outlet velocity in this investigation is varied by changing the pump output Q_{pu}.
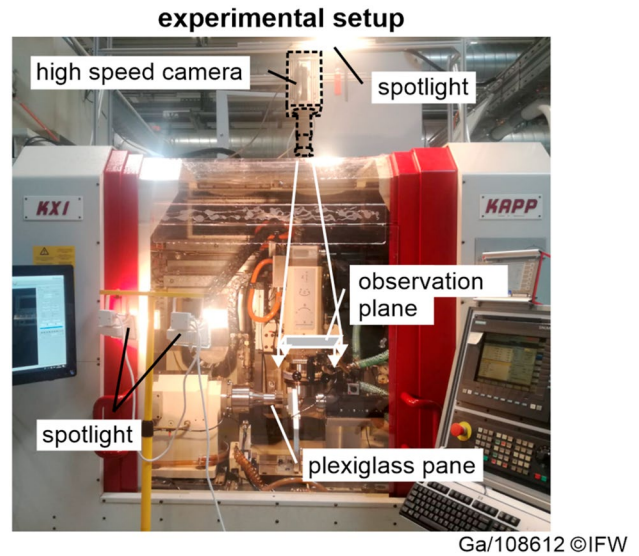
experimental setup

Ga/108612 ©IFW

Fig. 4 Experimental setup for the development of the coolant velocity sensor
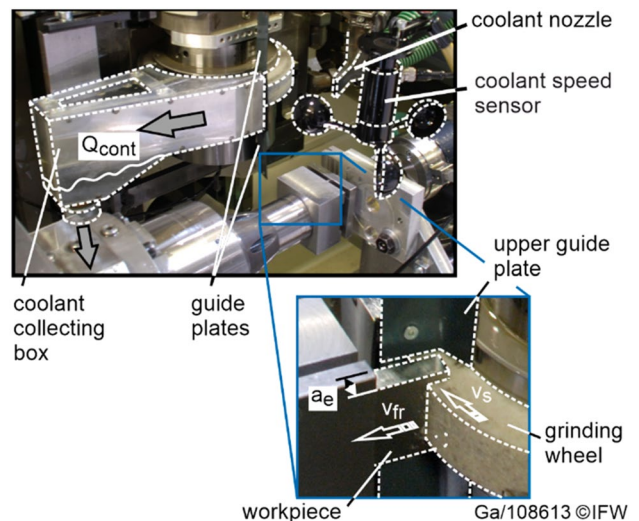

Ga/108613 ©IFW

Fig. 5 Experimental setup for collection of coolant within the KAPP KX1 machine tool

In order to examine the influence of coolant velocity on the grinding process, a collection box for coolant was further developed. With this box, it is possible to investigate the flow rate of coolant through the contact zone. The essential difference from previous units is the guidance of the coolant volume flow after collection [23, 24]. Figure 5 shows the coolant collection box and the coolant conduction system after the collection box. The collecting box was adapted to the small available machine space. Improved sealing of the box was achieved by replicating the curvature of the grinding wheel. This leads to a minimization of the error due to an entry of cooling lubricant into the box
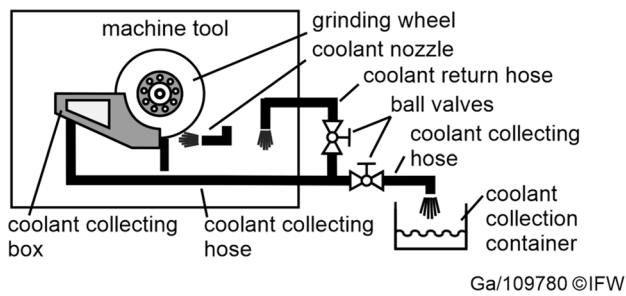
Fig. 6 Coolant guidance after the coolant collection box

that has not passed through the contact zone. In addition, guide plates were mounted on the side of the grinding wheel to support the sealing at this point. The conduction of coolant was realized with a hose system (diameter 1.5") so that there is a sufficiently large pipe cross-section that does not lead to a backup of coolant. This is led out of the machine tool and back in again in a loop (Fig. 6). A collecting tank was then provided outside the machine using a branch and two ball valves. During the beginning of the grinding process, both valves are closed, During the stationary tool engagement operation, the valve on the right hand side is openened for 20 s to collect the coolant through the contact area. Afterwards, the valve is shut again and the coolant flows through the coolant return hose back into the machine tool. The collected coolant is quantified by mass using a digital balance from the manufacturer Kern, type CXB 3K0.2. The resolution of the balance is 0.1 g. Before weighing, chips from the grinding process are filtered out of the collected coolant using filter fleece. In this way, the chips do not influence the weighing result incorrectly. The mass flow rate through the contact zone $\dot{m}_{cont}$ was then converted into a volume flow rate through the contact zone Q_{cont} by means of the density of the grinding oil used. In addition, the filtered chips are examined for their tempering color using a Keyence VHX-600 microscope. This enables a relative classification of the thermal load of the contact zone.

The grinding process for the examination of the coolant flow through the contact zone is plunge grinding. This process ensures constant feed conditions of the coolant into the contact zone on the one hand. On the other hand, this process allows a close range mounting of the collection box to the contact zone and thus a best possible collection of coolant after the contact zone.

The grinding parameters of this analogy test were chosen specifically so that they correspond to common cutting parameters in deep grinding ($a_e = 0.5$ mm, $d_{gw} = 200$ mm). Thus, the infeed was set to $a_e = 10$ mm, which corresponds to a common contact length in deep grinding. The radial feed rate was chosen based on the

equivalent chip thickness in deep grinding to $v_{fr} = 15$ mm/min, with a cutting speed of $v_s = 20$ m/s. As a grinding wheel a vitrified bond corundum tool from Saint Gobain Abrasive GmbH ($200 \times 30 \times 127$ IPA F60 HA20 VTX) is used, which is patterned by micro structures prior to each test. The coolant capacity can be increased locally by structuring the grinding wheel i.e. by means of a fly-cutting technique. By means of this process step the effective contact area was reduced to $A_{eff} = 75\%$.

3 Results and discussion

3.1 Influence of pump pressure and nozzle geometry on its outlet velocity

In order to investigate the influence of the primary nozzle geometry, each nozzle was tested at different pump pressures up to the maximum pressure of $p_{pu,max} = 24$ bar and the resulting coolant flow rate was recorded. The investigation was carried out with and without the secondary nozzle to isolate the influence of the primary nozzle. When investigating solely the primary nozzle, the secondary hose was sealed. Figure 7 shows the measured flow rates with and without the secondary nozzle at different pump pressure. It becomes evident, that the volume flow is overall much higher with the secondary nozzle attached, as this reduces the back pressure due to the larger overall outlet cross-section. With the secondary nozzle attached, the overall flow rate is mainly influenced by the primary nozzle, as the maximum pump pressure is the limiting factor. Additionally, the results show the influence of the primary nozzle's geometry. The flow rate increases with
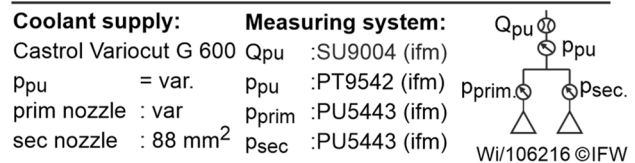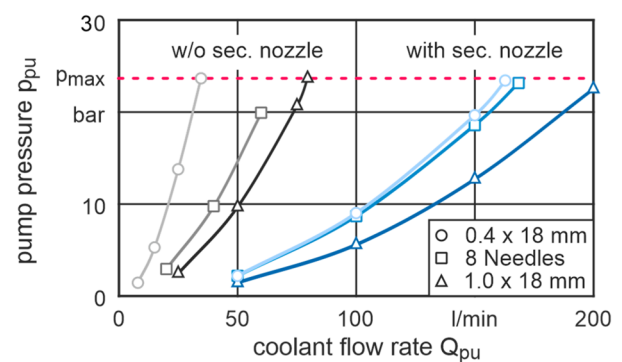

Fig. 7 Pump pressure and resulting flow rates for different primary nozzles with and without the secondary nozzle

the pump pressure for larger nozzle cross-sections for the flat-jet nozzles. The cross-section of the 0.4-nozzle is 60% smaller and results in a 57% lower flow rate. The influence of the nozzle type becomes evident in the comparison of the needle nozzle and the larger 1.0-mm flat-jet nozzle. Even though the cross-section of the needle nozzle is 33.

larger than the larger flat-jet nozzle, the resulting flow rate is 20% lower. This is due to the larger back pressure from the eight individual nozzles in comparison to a single outlet.

On the right hand side of Fig. 7, the flow rates of all nozzles are shown when simultaneously using the secondary spray nozzle with a cross-section of $A_{sec.} = 88$ mm^2. Not only is the coolant flow rate for this setup much higher but also is the influence of the primary nozzle's geometry even more apparent. The overall cross-section ($A = A_{prim.} + A_{sec.}$) with the needle nozzle is larger by 19% than the smaller flat-jet and by 7% larger than the larger flat-jet nozzle. However, the maximum volume flow of this setup is just 3.4% larger than that of the small and 16% lower than that with the large flat-jet.

With the spray nozzle and a split between the primary and secondary coolant hose, that is determined by the back pressure from each nozzle, the coolant pump can supply larger amounts of coolant to the cutting zone. The high back pressure from the needle nozzle results in lower overall flow rates, as lesser coolant flows through the primary nozzle.

With the presented Eq. (2) the measured overall flow rate Q_{pu} and partial nozzle pressures p_{prim} and p_{sec} are used to calculate the outlet velocity of the individual nozzles [Eq. (4) and (5)]. Figure 8 shows the calculated outlet velocities for varying nozzle setups and coolant flow rates. Here, the two flat-jet nozzles show the highest outlet velocities both with and without a secondary nozzle attached. The 0.4 mm nozzle shows the highest outlet velocity of $v_{cool} = 86.5$ m/s while the use of the 1.0 mm nozzle results in a maximum outlet velocity of 79.5 m/s., the needle nozzle delivers coolant to the contact zone with only 50% of the velocity of the 0.4-nozzle at $v_{cool} = 43.0$ m/s. Even though the flow rate (Fig. 7) is almost twice as high for this nozzle, the cross-section is with 350% significantly larger in comparison, which results in reduced outlet velocities.

$$Q = \frac{\dot{m}}{\rho} = Q_{pu} = A_{pu} \cdot c_{pu} = A_{prim.} \cdot c_{prim} + A_{sec.} \cdot c_{sec.} = \text{const.}$$

(4)

$$c_{nozzle} = \sqrt{c_{pu}^2 + \frac{2}{\rho}\left(p_{pu} - p_{nozzle}\right) + 2g\left(z_{pu} - z_{nozzle}\right)}$$ (5)

Similar results are visible when using the secondary nozzle. The flow rates are majorly increased, as was
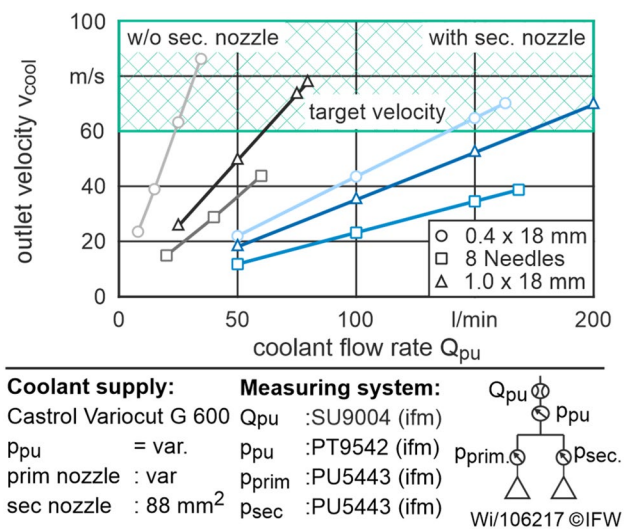

Fig. 8 Coolant flow rates and resulting outlet velocities for different nozzle setups

shown previously. The blue graphs in Fig. 8 (right) depict only outlet velocities of the three different primary nozzles. Here it becomes evident, that both flat-jet nozzles result in high velocities of about 70 m/s. Due to the different cross-sections, the larger 1.0-nozzle delivers an increase in flow rate of about 22%. Both nozzles, with and without the use of a secondary nozzle are able to lubricate the contact area, as they reach the required outlet velocity of $v_{cool,min} = 0.6 \cdot v_s = 60$ m/s. However, the 1.0-flat-jet nozzle is better suited to cool the process as it results in a higher overall coolant flow rate to remove chips and heat from the contact area. The needle nozzle is unsuited for the application in high-speed grinding as its internal back pressure results in lower flow rates and outlet velocities than the flat-jet nozzles.

3.2 Influence of nozzle outlet velocity on the coolant flow through the contact zone

In the first step of this part of the investigation, a coolant velocity sensor was developed based on an anemometer. This sensor enables a direct measurement of the coolant velocity. The calculation as an indirect measurement method highly depends on the quality of the measurements and does not regard the change in velocity between the nozzle outlet and the contact area.

Compared to other anemometer sensors, the decisive factor in the selection of this sensor was the measuring range in air of up to 50 m/s and the protection class IP65 according to DIN EN 60529 [27]. This range covers the usual range of cutting speeds for the use of conventional grinding processes. Protection class IP65 corresponds to protection against dust as well as against water jets from

a nozzle at any angle. In conventional use, the sensor is completely surrounded by the driving medium air. For this application, the output signal of the sensor is calibrated by a linear sensitivity. However, when used inside the machine tool, the driving medium is oil, which only partially interferes with the blades of the sensor. Due to the change in fluid flow, the output signal of the sensor has to be calibrated for the new application. This is done using a high speed camera positioned above the machine (Fig. 4). For this application, the positioning of the sensor in relation to the coolant beam must be taken into account. Based on the evaluated video data, it was observed that the engagement of the blades in the coolant beam should be tangential, similar to Fig. 9. An increased engagement slows the sensor at the entrance of the blade into the coolant beam and thus leads to a reduced measuring signal.

Utilizing the recorded video data, it was possible to measure the velocity of individual traceable drops of coolant by measuring the path and time (Fig. 9). Figure 10 shows the measurement results on the left side on an example of one coolant flow speed. The measured coolant velocity v_{cool} is calculated as the mean value of the individual drop speeds. The coolant velocities measured in this way were then compared to the respective measured voltage of the output signal U_a.

For the determination of a sensitivity characteristic, the coolant flow was varied in five steps by changing the coolant pump pressure Q_{pu}. The corresponding results are shown in Fig. 10 on the right. The sensitivity was calculated as linear regression since the manufacturer specifies the sensor behaviour as linear. The boundary condition of the regression was set to $v_{cool} = U_a = 0$. The resulting, determined sensitivity is 3.49 m/(s·V). Thus, the

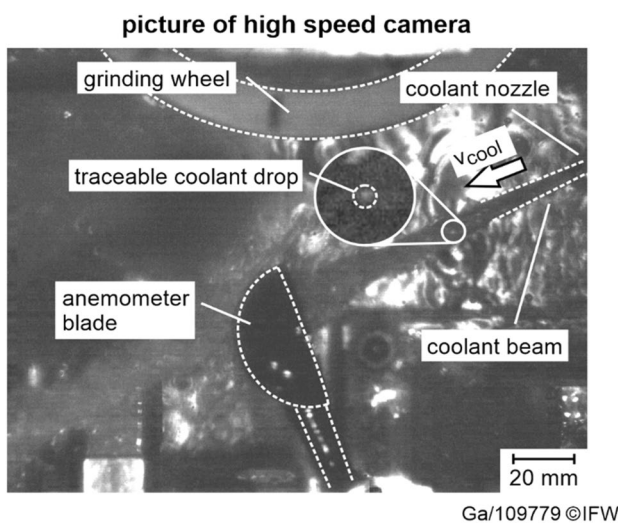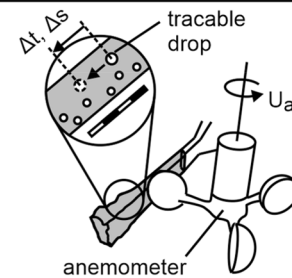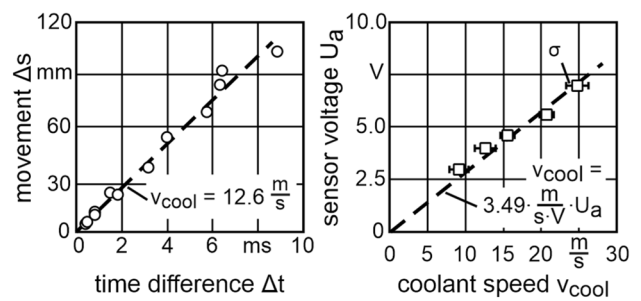| coolant		measurement equipment	
type:	Oil	anemometer:	PCE-FST 200-201
Q_{pu}	= var.	camera:	Photron Fastcam SA5
nozzle cross		time resolution:	12,000 1/s
section	= 103 mm^2		Ga/108614 ©IFW

Fig. 10 Measurement results of the tracing of coolant drops by means of a high speed camera

maximum coolant velocity that can be measured with this sensor is 34.9 m/s.

In order to determine the influence of the coolant velocity on the volume flow of coolant through the contact zone, the coolant was collected in a coolant collection box. The measurement results on the influence of the cooling lubricant velocity on the cooling lubricant volume flow show a strong dependence in the following way. A maximum of the volume flow occurs when the coolant velocity corresponds to the circumferential speed of the grinding wheel (Fig. 11). A reduction, as well as an increase in the coolant velocity, leads to a decrease in the coolant volume flow through the contact zone. The reason for this is that the coolant does not need to be accelerated or decelerated to penetrate the pores of the grinding tool.

The results of these investigations also show that the coolant flow rate through the contact zone has an influence on the temperature in the contact zone. The tempering colours of the collected grinding chips are brown to blue if the coolant velocity does not correspond to the circumferential speed of the grinding wheel (Fig. 11, bottom) [28]. If both speeds are equal, there is no tempering colour, which indicates a lower thermal load in the contact zone. This result supports that state of the art of an ideal ratio of $v_{cool}/v_s = 0.6$–1.0.
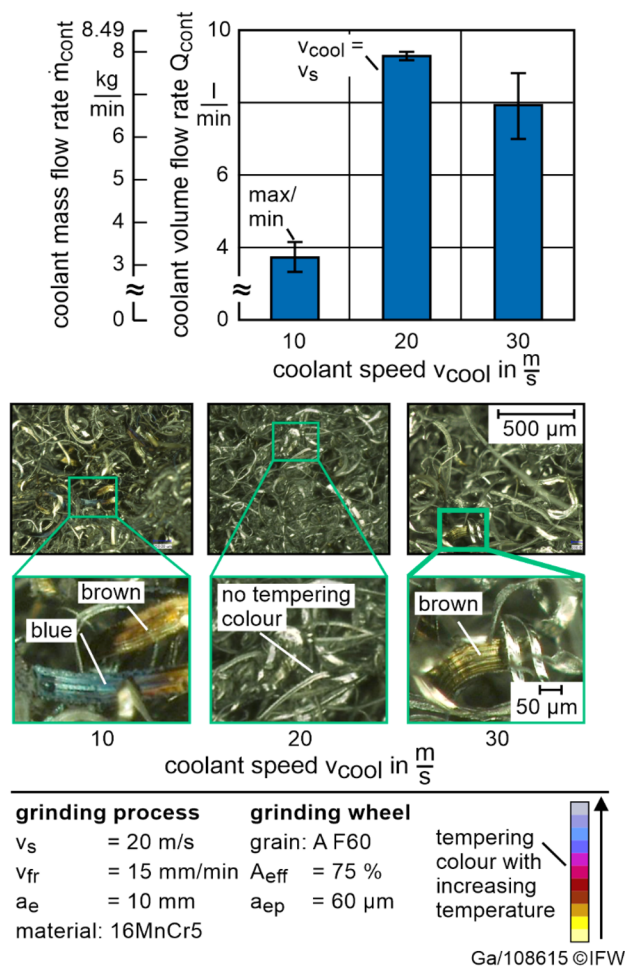

Fig. 9 Representative picture of the high-speed camera

Fig. 11 Influence of the coolant velocity on the resulting coolant flow rate through the contact zone with according chips

4 Conclusions and outlook

The cooling of grinding processes is a key aspect to increase productivity while securing the surface quality. For existing machine tools, the supply of coolant to the contact zone is the primary optimization approach. Throughout this paper, two different methods to influence and determine the coolant outlet velocity were shown.

For high-performance grinding processes, the coolant velocity is calculated by means of measured nozzle cross-sections and pressure values as well as an overall volume flow rate. With the use of pressure and flow rate sensors, the outlet velocities and flow rates were calculated for varying nozzle setups. With this calculation, the coolant conditions can be adjusted to the process needs. From the results, it was proven that the change in coolant hose pressure has a high impact on the overall system. The outlet velocity is, however, not solely dependent on the cross-section of the nozzle but also the type of nozzle. Due to high back pressure, the needle nozzle

was not able to deliver high quantities or velocities of coolant to the contact zone even though the cross-section was larger than that of the flat-jet nozzles. With flat-jet nozzles, it was possible to achieve a coolant outlet velocity for high-performance grinding that met the requirements from the literature of $v_{cool} \geq 0.6 \, v_c$.

Additionally, a measuring system was designed for the direct measurement of the outlet velocity by means of an adapted anemometer. The sensor was calibrated for the measurement of oil outlet velocities via high-speed camera observations. In order to examine the influence of the coolant velocity on the volume flow through the contact area, a coolant collecting box was designed and implemented into a machine tool. From the results, it can be seen that a maximum volume flow was achieved at a coolant velocity equal to the cutting speed. With the high volume flow through the contact area, the tempering colours of the resulting chips indicate a low thermal load on the contact zone due to the tailored coolant condition.

The main findings of this paper include the following:

1. Pressure and flow rate sensors can be integrated into existing machine tools to accurately tailor the coolant supply to the process` demand.
2. Coolant outlet velocities equal to the tool cutting speed lead to a maximum amount of coolant through the contact area and thereby a maximum reduction of grinding temperature.
3. Flat-jet nozzles are better suited for high-performance grinding operations as they offer higher outlet speeds compared to needle nozzles. The needle nozzle results in an outlet velocity reduction of about 50% while providing a larger cross-section of 71%.

The presented results enable the industrial application of the measurement system to improve the coolant conditions of a wide variety of grinding processes. Used with the results from Zhao [21] the system enables industrial and scientific applications for the optimization of high-performance grinding operations. Further scientific investigations will focus on the influence of the tailored coolant supply on the grinding behaviour and tool life. Especially the influence of the coolant flow rate through the contact area and its effect on the grinding and chip temperature offers promising approaches for further studies. In conclusion, the optimization approaches of this paper require little effort for applicants to tailor the coolant conditions of their grinding processes. Especially for existing machine tools, these approaches can secure an optimal coolant outlet velocity and thus low thermal loads on the grinding process.

Declarations

Conflict of interest The authors declare no conflict of interest.

References

1. Klocke F (2009) Manufacturing processes 2: grinding. Springer-Verlag, Berlin Heidelberg, Berlin, Heidelberg Honing, Lapping. https://doi.org/10.1007/978-3-540-92259-8

2. Tawakoli T, Westkämper E, Rabiey M, Rasifard A (2007) Influence of the type of coolant lubricant in grinding with CBN tools. Int J Mach Tools Manuf 47(5):734–739

3. Brinksmeier E (1991) Prozess- und Werkstückqualität in der Feinbearbeitung. VDI-Verl, Düsseldorf

4. Dröder K, Hoffmeister H-W, Bayoumi I, Seidel C (2016) Schleifen unter Einsatz von Minimalmengenschmierung und flüssigem Stickstoff (MMS-LN2). In: Denkena B, Hoffmeister H-W (Hrsg). Jahrbuch Schleifen, Honen, Läppen und Polieren: Verfahren und Maschinen, 67th ed. Vulkan. Essen

5. Alberts M, Kalaitzidou K, Melkote S (2009) An investigation of graphite nanoplatelets as lubricant in grinding. Int J Mach Tools Manuf 49(12–13):966–970. https://doi.org/10.1016/j.ijmachtools.2009.06.005

6. Hoffmeister H-W (2012) Innovative Ansätze für das Kühlen beim Schleifen. in Tawakoli T (Hrsg.). Moderne Schleiftechnologie und Feinstbearbeitung 2012: Neue Entwicklungen und Trends aus Forschung und Praxis ; 9. Seminar "Moderne Schleiftechnologie und Feinstbearbeitung" am 15.05.2012 in Stuttgart. Hochsch. Furtwangen, Abt. Villingen-Schwenningen. Villingen-Schwenningen

7. Industrieverband e.V. (2009) Raumluftüberwachung bei der Anwendung von Gasen, Köln

8. Brinksmeier E (2016) Thermal Management of Grinding Processes, Aachen

9. Heinzel C (1999) Methoden zur Untersuchung und Optimierung der Kühlschmierung beim Schleifen, Dr.-Ing. Dissertation. Shaker, Aachen

10. Vesali A (2015) Hochleistungs-/Hochgeschwindigkeitsschleifen mit laserstrukturierten CBN-Schleifscheiben, Dr.-Ing. Dissertation. Albert-Ludwigs-Universität Freiburg, Freiburg. https://d-nb.info/112957265X/34

11. Davies TP, Jackson RG (1981) Air flow around grinding wheels. Precis Eng 3(4):225–228. https://doi.org/10.1016/0141-6359(81)90097-0

12. Brinksmeier E, Heinzel C, Wittmann M (1999) Friction, cooling and lubrication in grinding. CIRP Ann 48(2):581–598. https://doi.org/10.1016/S0007-8506(07)63236-3

13. Treffert C (1995) Hochgeschwindigkeitsschleifen mit galvanisch gebundenen CBN-Schleifscheiben, Dr.-Ing. Dissertation. Technische Hochschule Aachen, 1994. Shaker, Aachen

14. Gviniashvili VK, Woolley NH, Rowe WB (2004) Useful coolant flowrate in grinding. Int J Mach Tools Manuf 44(6):629–636. https://doi.org/10.1016/j.ijmachtools.2003.12.005

15. Okuyama S, Nakamura Y, Kawamura S (1993) Cooling action of grinding fluid in shallow grinding. Int J Mach Tools Manuf 33(1):13–23. https://doi.org/10.1016/0890-6955(93)90060-8

16. Saxler W, Stabauer R (2020) Einfluss des umlaufenden Luftpolsters an rotierenden Schleifscheiben auf die Kühlschmierstoff-Zufuhr. Dihw - Diamant Hochleistungswerkzeuge 1:32–37

17. Heinzel C, Meyer D, Kolkwitz B, Eckebrecht J (2015) Advanced approach for a demand-oriented fluid supply in grinding. CIRP Ann 64(1):333–336. https://doi.org/10.1016/j.cirp.2015.04.009

18. Brinksmeier E, Geilert P (2018) Bedarfsgerechte Kühlschmierstoff-Zufuhr beim Verzahnungsschleifen. In: Azarhoushang B (Hrsg) Moderne Schleiftechnologie und Feinstbearbeitung

19. Ott HW (2002) Richtig gekühlt ist halb geschliffen - eine eher physikalische Betrachtung. In: Tawakoli T (Hrsg) Moderne Schleiftechnologie und Feinstbearbeitung: Neue Entwicklungen und Trends aus Forschung und Praxis ; 4. Seminar „Moderne Schleiftechnologie" am 25.04.2002 in Villingen-Schwenningen. Fachhochsch. Furtwangen Abt. Villingen-Schwenningen. Villingen-Schwenningen, S. pp 701–732

20. Schnödt J, Schrottner G, Storr M, Bausch K (2012) Energieeffizientes Schleifen (Zwischenbericht). In: Tawakoli T (Hrsg) Moderne Schleiftechnologie und Feinstbearbeitung 2012: Neue Entwicklungen und Trends aus Forschung und Praxis ; 9. Seminar "Moderne Schleiftechnologie und Feinstbearbeitung" am 15.05.2012 in Stuttgart. Hochsch. Furtwangen, Abt. Villingen-Schwenningen

21. Zhao Z, Qian N, Fu Y (2022) Coolant condition and spindle power in high-efficiency-deep-grinding of nickel-based superalloy profile part. Mater Manuf Process 37(9):1022–1034. https://doi.org/10.1080/10426914.2021.2001516

22. Helpertz M, Wenderott D (2017) Pumpenauswahl und Betriebsbedingungen bei Schleifanwendungen. 14. Hanser Schleiftagung: Schleifprozesse: sicher, reproduzierbar, effizient! Hanser. München

23. Batchelor GK (2010) An introduction to fluid dynamics, 1st edn. Cambridge University Press, Cambridge. https://doi.org/10.1017/CBO9780511800955

24. PCE Deutschland GmbH (2018) Datenblatt Windsensor PCE-FST 200-201, Meschede

25. Göttsching T (2017) Schleifen von aluminiumhaltigem UHC-Stahl, Dr.-Ing. Dissertation. Leibniz Universität Hannover, TEWISS Verlag, Garbsen

26. Brinksmeier E (2006) Kostenreduzierung beim Schleifen durch eine angepasste Kühlschmierstoffversorgung: IGF-Vorhabennummer: 14167 N/1. Bremen, Universität Bremen, Institut für Werkstofftechnik, Abschlussbericht

27. DIN - Deutsches Institut für Normung e.V. (2019) Schutzarten durch Gehäuse(DIN EN 60529). Beuth Verlag GmbH, Berlin
28. Welsch N, Liebmann CC (2012) Farben: natur technik kunst, 3rd edn. Spektrum Akademischer Verlag, Heidelberg

Publisher's Note Springer Nature remains neutral with regard to jurisdictional claims in published maps and institutional affiliations.